On spatio-temporal message diffusion in epidemic broadcasting

KOHEI WATABE[1]*†, HIROYUKI OHSAKI[2]

[1] *Graduate School of Information Science and Technology, Osaka University, Japan*
[2] *Department of Informatics School of Science and Technology, Kwansei Gakuin University, Japan*

Received 17 December 2004; In final form 1 April 2005

Although there have been many analyses of the effects of node mobility on communication performance of DTNs (Delay/Disruption-Tolerant Networks), to the best of our knowledge, there is no research investigating the impact of local positional distributions of nodes. In this paper, we analyze the effect of locality of node mobility on the spatio-temporal message diffusion in epidemic broadcasting in DTNs. We assume that each node has its own anchor point and that each node tends to move around the anchor point. By representing the strength of locality of node mobility through the shape of the positional distributions of nodes, we derive the dynamics of the spatio-temporal message diffusion in epidemic broadcasting. Through numerical examples, we show that communication performance is significantly affected by the tail of the pdf (probability density function) of node position. We derive a positional distribution for the Homesick Lévy Walk mobility model, which is a representative model with locality of node mobility, and derive the delivery time in epidemic broadcasting.

Key words: Delay/disruption-tolerant network, Mobile ad-hoc network, Epidemic broadcasting, Locality, Message diffusion, Mobility

* email: k_watabe@vos.nagaokaut.ac.jp
† Corresponding author. He is currently on Graduate School of Engineering, Nagaoka University of Technology, Japan.

1 INTRODUCTION

In recent years, DTNs (Delay/Disruption-Tolerant Networks) composed of mobile nodes have attracted considerable attention. The DTN architecture enables the communication on MANET (Mobile Ad-hoc NETwork), in which nodes are sparse and end-to-end connectivity is not likely to be achievable. It is anticipated that this approach will be useful for networks in disaster areas, military networks, interplanetary networks, sensor networks, and so forth. Many researchers have proposed algorithms for achieving communication in DTNs composed of mobile devices [4, 14, 22, 1, 24, 13, 21, 25], and most of them adopt store-and-carry message forwarding to compensate for the lack of end-to-end connectivity.

Though one-to-one communication has been actively studied in the field of DTNs, one-to-all communication is also important in the field. One-to-all communication has several applications, e.g., delivering advertisements of available services, distributing software updates, spreading acknowledgements, etc. In a part of DTNs, a node frequently joins (or leaves) the network. Especially, in such DTNs, it is expected that one-to-all communication will be actively used since it is difficult to maintain the node list of the network it joins for each node.

To realize one-to-all communication, DTNs can utilize epidemic broadcasting [6], where nodes carrying a message (infected nodes) forward a copy of the message when they enter the communication range of nodes that do not have the message (susceptible nodes). As a message is repeatedly forwarded by infected nodes, it diffuses message over nodes in the network and the spatial distribution of infected nodes becomes wider. Several algorithms for epidemic broadcasting have been proposed, and their performances in terms of message delivery time, coverage, and the number of duplicate messages have been analyzed [7, 9, 8].

Generally, node mobility affects the communication performance of DTNs when nodes communicate through store-and-carry message forwarding. In the literature, several analyses of the effects of node mobility have been conducted. Message delivery time and throughput have been compared under different mobility models, including complex ones that impose constraints on the mobility of nodes [17, 6, 27], as in the case of vehicles on a road, in addition to simple ones, such as the RWP (Random WayPoint) mobility model [10], the RD (Random Direction) mobility model [19] and the RW (Random Walk) mobility model. Moreover, the effects of the distribution of rectilinear movement distance on message delivery time, buffer utilization,

and throughput for one-to-one communication have been analyzed using a mobility model in which nodes repeatedly perform rectilinear motion and randomly change the direction of motion [12, 18]. The effects of heterogeneity of node mobility on message delivery time have also been explored [16].

Although there have been many analyses of the effects of a mobility model on the communication performance of DTNs, to the best of our knowledge, there has been no research investigating the impact of local positional distributions of nodes to understand the spatio-temporal message diffusion in epidemic broadcasting. As shown in Figure 1(a), the trajectories of nodes, which are likely to move around within a specific area on a field, are less likely to intersect, and the diffusion of messages is slow because the frequency of contact between nodes is very low. However, in the works mentioned above, the areas in which nodes can move are assumed to be equal (see Figure 1(b)), and the mobility models generate node trajectories whose stationary positional distributions are identical. For instance, in [17], the movement of each node is restricted to a grid and the stationary positional distribution is the same for all nodes since they move under the same restrictions. Moreover, in the mobility models in [12, 18], nodes are uniformly distributed over a field in a steady state.

It is important to analyze message diffusion for epidemic broadcasting in environments in which node mobility is localized and nodes are distributed locally on a field. For instance, when nodes forming a DTN correspond to humans, their movement should be centered at certain points on a field since it is assumed that humans tend to move around the bases of their activity (e.g., their home or office). Fujihara *et al.* proposed the HLW (Homesick Lévy Walk) mobility model, in which each node has its own anchor point and the nodes are locally distributed [5]. The HLW mobility model can reproduce the properties that are observed in real GPS (Global Positioning System) trace data. They analyzed the reachability of messages in a DTN composed of nodes with finite buffers.

In this paper, we analyze the effects of the locality of node mobility on spatio-temporal message diffusion in epidemic broadcasting. We represent the strength of locality of node mobility through the shape of the positional distributions of nodes and reveal the relation between positional distribution and frequency of contact between nodes. In this way, we derive a weighted adjacency matrix A whose elements are the expected frequencies of contact between each pair of nodes, which enables mapping from the problem of epidemic broadcasting for mobile nodes to the problem of epidemics on a graph. Numerically solving the dynamic equation of epidemics on a graph,

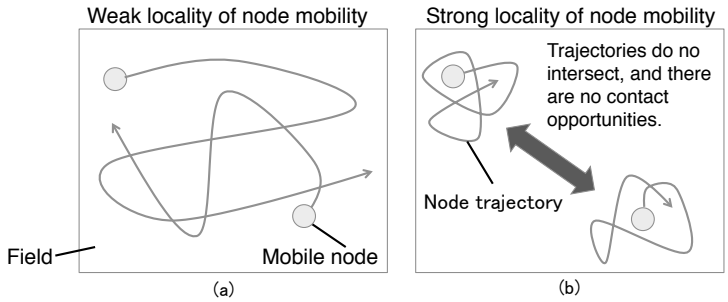

FIGURE 1
Strength of locality of node mobility and contact frequency.

we compare message diffusion speed for various shapes of the positional distribution of nodes. We clarify the effects of the shape, including tail behavior, on message delivery time and the spatial diffusion of infected nodes. Additionally, we derive a positional distribution of a node that moves according to the HLW mobility model as a representative mobility model that includes locality of node mobility and derive message delivery time.

The rest of the paper is organized as follows. In Section 2 we briefly describe existing mobility models and explain the concept of locality of node mobility. In Section 3, we then derive the message delivery time and the infection probability of nodes. In Section 4, using numerical experiments, we investigate the effects of the shape of the positional distribution of nodes on message delivery time and the spatial diffusion of messages. In Section 5, we analyze message delivery time in the HLW mobility model. Finally, we conclude this paper and discuss future works in Section 6.

2 NODE MOBILITY AND LOCALITY

In order to analyze communication performance on MANETs, various mobility models including the RW, RWP, and RD mobility models have been proposed [2, 18, 5]. In the following, we briefly summarize those models.

- **RW (Random Walk) mobility model:** The RW mobility model is one of the most primitive mobility models. In this model, each node randomly selects its direction and velocity and travels in a straight line.

The selection of direction and velocity is repeated after a prescribed time t or length l, and reflection occurs at field boundaries.

- **RWP (Random WayPoint) mobility model:** In simulations of MANETs, the RWP mobility model is one of the most popular mobility models. In this model, each node randomly selects its destination in a field and travels straight to that destination at a constant velocity which is randomly selected from a uniform distribution. When it reaches the destination, it waits there for a randomly chosen time and then selects a new destination and velocity.

- **RD (Random Direction) mobility model:** A node that follows the RD mobility model travels in a straight line and waits for a randomly chosen time once it reaches a field boundary. Then, it randomly selects a new direction and travels straight to another field boundary. In the modified RD mobility model [19], occasionally each node waits and selects a new direction before it reaches the field boundary. The movement pattern is similar to that of the RW mobility model.

- **LW (Lévy Walk) mobility model:** In the LW mobility model, each node has the same movement pattern as in the RW mobility model except that the flight length l follows a power law distribution. If flight length l has a power law distribution $f(l) \sim l^{-\beta}$, the variance of flight length diverges when $\beta \leq 3$ and the expectation diverges when $\beta \leq 2$. By using GPS trace data, Rhee *et al.* [18] showed that the flight length of human mobility follows a power law with $1.35 \leq \beta \leq 2.40$.

- **HLW (Homesick Lévy Walk) mobility model:** The HLW mobility model is an extended version of the LW mobility model. In the HLW mobility model, each node has its own anchor point to which it returns after a flight with probability $\alpha\,(0 \leq \alpha \leq 1)$. The directions and lengths of flights are chosen as in the LW mobility model. The HLW mobility model reduces to the LW mobility model when $\alpha = 0$. The HLW mobility model exhibits power laws for both inter-contact times and flight lengths [18, 5].

The HLW mobility model is a representative model in which a node has a localized distribution in a stationary state. A node that follows the RD, RW, or LW mobility models has a uniform distribution over the whole field in a stationary state. A node that follows the RWP mobility model rarely passes near the edges of a field, and the pdf (probability density function) $p(x, y)$ of

node position is approximately given by the following equation [23].

$$p(x,y) \simeq \frac{36}{S^3}\left(x^2 - \frac{S}{4}\right)\left(y^2 - \frac{S}{4}\right),$$

where S denotes the area of the field on which nodes can move. Nodes may exist on most part of the field except the edges and are widely distributed over a field, though the distribution is not a uniform distribution. In contrast, the HLW mobility model explicitly includes locality of node mobility when the return probability α is nonzero.

We represent the locality of node mobility by the shape of the stationary positional distributions of nodes. This allows us to consider a wide variety of node mobilities. The anchor point of a node is represented by the mean point (it is represented by the mode point if mean cannot be defined) and we quantify the strength of locality of node mobility as the expectation $\mathrm{E}[L]$ of the distance L from the mean (or mode) position to the current node position. Larger values of $\mathrm{E}[L]$ indicate a wider range of motion of nodes and weaker locality.

3 ANALYSIS AND NETWORK MODEL

In this section, we present our network model, model the locality, and derive the contact frequency of nodes from these positional distributions. We then derive message delivery time and the infection probability of a node in epidemic broadcasting from the contact frequency. In the derivation, we construct a weighted adjacency matrix whose elements are contact frequencies, thereby mapping the problem of epidemic broadcasting for mobile nodes to the problem of epidemics on a graph.

3.1 Network Model

The model we use in the paper is based on Unit Disc Graph (UDG) [3]. In UDG, a node can forward a message only when the distance between the node and a receiver node is communication range r or less. Two nodes are said to be in contact (i.e., can communicate) when they are within the communication range of both nodes. UDG can be defined in Euclidean space. As we mentioned above, in most MANET/DTN research, the main consideration is communication performance on a two-dimensional Euclidean space. Our main focus is message diffusion on a two-dimensional space, though we consider message diffusion on one- and two-dimensional spaces in the experiments. Although a DTN that is composed of nodes on a one-dimensional space is unrealistic, these analyses give some insights into spatial diffusion.

We assume that nodes $i\,(i = 1, 2, \ldots, N)$ moves on the field, and they have stationary positional distributions. Therefore, the topology of our network model that is based on UDG is dynamically changes, since we express mobility of node. We assume that nodes travel on a straight line while they are in contact (a node does not change the direction when it is in a communication range of another node). In our model, an infected node always forwards a message when it is in contact with a susceptible node. Note that we assume that infected nodes forward the message instantly, and we do not take message size into account. Our model can be easily extended to include probabilistic infection. Additionally, we assume that any performance deterioration due to interference of radio communication is negligible.

3.2 Derivation of Contact Frequency

In order to derive the message delivery time in epidemic broadcasting, we first derive the frequency of contact between nodes from the stationary positional distribution of the nodes. In DTNs, contact frequency strongly affects the performance of epidemic broadcasting since infected nodes forward and diffuse messages only when they are in contact with other nodes. We let $p_i(x)$ denote the pdf of the position of node i on a one-dimensional space. When nodes move along a one-dimensional space, by using the pdf $p_i(x)$ for the position of node i, we can express the total contact duration T_{total} per unit time for nodes i and j as

$$\begin{aligned} T_{\mathrm{total}} &= \int_{-\infty}^{\infty} p_i(x) \int_{x-r}^{x+r} p_j(y)\mathrm{d}y\mathrm{d}x \\ &\simeq 2r \int_{-\infty}^{\infty} p_i(x)p_j(x)\mathrm{d}x, \qquad \text{for sufficiently small } r. \end{aligned} \tag{1}$$

When nodes move on a two-dimensional space, by using the pdf $p_i(x, y)$ for the position of node i, we can similarly express T_{total} as

$$\begin{aligned} T_{\mathrm{total}} &= \int_{-\infty}^{\infty} \int_{-\infty}^{\infty} p_i(x, y) \int\int_{R_{x,y}} p_j(z, w)\mathrm{d}z\mathrm{d}w\mathrm{d}x\mathrm{d}y \\ &\simeq r^2\pi \int_{-\infty}^{\infty} \int_{-\infty}^{\infty} p_i(x, y)p_j(x, y)\mathrm{d}x\mathrm{d}y, \\ &\qquad\qquad \text{for sufficiently small } r, \end{aligned} \tag{2}$$

where $R_{x,y}$ denotes the inside area of a circle with a center (x, y) and a radius r.

Provided that contact duration is independent of the number of contacts per unit time, we can derive the relation between the total contact duration

$T_{\rm total}$ per unit time and the contact frequency $w_{i,j}$ for nodes i and j from the average contact duration $T_{\rm cd}$ per contact as

$$w_{i,j} = \frac{T_{\rm total}}{T_{\rm cd}}. \tag{3}$$

When nodes move on a one-dimensional space, $T_{\rm cd} = 2r/\bar{v}$, where $\bar{v}$ denotes the average relative velocity of nodes. When nodes move on a two-dimensional space, it is not trivial to derive the average contact duration $T_{\rm cd}$ because of variation in the direction of node movement. Samar *et al.* [20] have investigated the duration of contact between mobile nodes and obtain the average duration of contact $T'_{\rm cd}(v)$ between a node with velocity v and other nodes by assuming that the velocities of other nodes have uniform distribution $U(v_{\min}, v_{\max})$. Then,

$$\begin{aligned} T'_{\rm cd}(v) = {} & \frac{r}{2(v_{\max} - v_{\min})} \int_0^{\pi} \log \left| \frac{v_{\max} + \sqrt{v_{\max}^2 - v^2 \sin^2 \phi}}{v + v \cos \phi} \right| {\rm d}\phi \\ & - \frac{r}{2(v_{\max} - v_{\min})} \int_{\phi_0}^{\pi} \log \left| \frac{v_{\min} + \sqrt{v_{\min}^2 - v^2 \sin^2 \phi}}{v_{\min} - \sqrt{v_{\min}^2 - v^2 \sin^2 \phi}} \right| {\rm d}\phi, \end{aligned}$$

where $\phi_0 = \pi - \sin^{-1}(v_{\min}/v)$. If we assume that v also obeys a uniform distribution $U(v_{\min}, v_{\max})$, we obtain

$$T_{\rm cd} = \frac{1}{v_{\max} - v_{\min}} \int_{v_{\min}}^{v_{\max}} T'_{\rm cd}(v) {\rm d}v. \tag{4}$$

As a result, for a one-dimensional space, we can derive the contact frequency for any arbitrary node pair by substituting Eqs. (1) and (4) into Eq. (3). We can also derive it by substituting Eqs. (2) and (4) into Eq. (3) for a two-dimensional space.

We can map the problem of epidemic broadcasting for mobile nodes with a stationary positional distribution p_i to the problem of epidemics on a graph G associated with a weighted adjacency matrix with elements $w_{i,j}$ since the rate at which an infected node i forwards a message to a susceptible node j is given by the frequency of contact $w_{i,j}$ between nodes i and j. The weighted adjacency matrix of graph G is defined as

$$A = \begin{pmatrix} 0 & w_{2,1} & \cdots & w_{N,1} \\ w_{1,2} & 0 & & w_{N,2} \\ \vdots & & \ddots & \vdots \\ w_{1,N} & w_{2,N} & \cdots & 0 \end{pmatrix},$$

where N denotes the number of nodes.

3.3 Derivation of Message Delivery Time and the Infection Probability of a Node

If the contact frequency is w for every node pair, the ratio of node infection at time t, $I(t)$, satisfies the differential equation [28]:

$$\frac{\mathrm{d}}{\mathrm{d}t}I(t) = wI(t)(1 - I(t)). \tag{5}$$

This model is similar to the SI (Susceptible-Infected) model [15], which is a well-known model of the diffusion of an infectious disease in the field of mathematical epidemiology. The solution of Eq. (5) is the logistic curve

$$I(t) = \frac{1}{1 + (N-1)\mathrm{e}^{-wNt}}. \tag{6}$$

The assumptions of the SI model are as follows [15]: 1) Every node is either susceptible or infected node, and a susceptible node changes into an infected node when it contacts another infected node; 2) Every node has an equal chance, per unit time, of coming into contact with every node; 3) Nodes contact completely at random (i.e., inter-contact time follows exponential distribution, and contact events of each node pair independently occur).

Using the weighted adjacency matrix A that we derived in the previous subsection and assuming that contact times are independent of each other, we can derive the following difference equation for the probability $\pi_i(t)$, which is defined as the probability of infection of node i at time t.

$$\boldsymbol{\pi}(t + \Delta t) = (E - \Pi)\, A\, \boldsymbol{\pi}(t)\Delta t + \boldsymbol{\pi}(t), \tag{7}$$

$$\boldsymbol{\pi}(t) = \begin{pmatrix} \pi_1(t) \\ \pi_2(t) \\ \vdots \\ \pi_N(t) \end{pmatrix},$$

$$\Pi = \begin{pmatrix} \pi_1(t) & 0 & \cdots & 0 \\ 0 & \pi_2(t) & & 0 \\ \vdots & & \ddots & \vdots \\ 0 & 0 & \ldots & \pi_N(t) \end{pmatrix},$$

where E denotes the identity matrix of dimension N. We assume that nodes contact completely at random as with the SI model although we do not assume

that every node has an equal chance, per unit time, of coming into contact with every node. Though a calculation result of $I(t)$ depends on accuracy of T_{cd} in our analysis, it does not affect scaling law of message diffusion speed since $I(t)$ is inversely proportional to T_{cd}. Note that Eq. (7) is a natural extension of Eq. (5). By numerically solving the difference equation of Eq. (7), we can derive the infection probability $\pi_i(t)$ of node i at time t. The ratio of infected nodes at time t is calculated from $\boldsymbol{\pi}(t)$ as

$$I(t) = \frac{1}{N} \sum_{i=1}^{N} \pi_i(t). \tag{8}$$

We can thus derive the ratio $I(t)$ of infected nodes at an arbitrary time t, and obtain the period that is needed to deliver a message (the message delivery time).

Note that the message delivery time obtained by this approach is an approximation due to the nature of the SI model. In the SI model, there is an assumption that nodes contact completely at random. We likewise assume it in our model. Therefore, the probability that message forwarding from node i to node j occurs is the product of the probabilities of the two events that node i is infected and that node j is susceptible. However, precisely speaking, we should express the probability of message forwarding as $\pi_i(t)(1 - \pi_j(t)) + c$ with some constant c, since the event that node i is infected and the event that node j is susceptible are not independent. Generally, if node i is infected, the probability that node j is susceptible tends to be small. Therefore, $c < 0$ and the delivery time derived by our approach gives a lower bound. We will confirm this by the numerical experiments in Section 4.

4 NUMERICAL EXPERIMENTS

Using Eq. (7) to derive message delivery time and the infection probability of each node, we investigate the effect of the shape of the positional distributions p_i of nodes on the communication performance of epidemic broadcasting by giving examples of positional distributions of nodes. First, assuming that p_i is one- or two-dimensional normal distribution, we investigate the effects of the strength of locality of node mobility. Next, assuming that p_i is one- or two-dimensional Cauchy distribution, we investigate the effects of the tail behavior of the positional distribution.

4.1 Effect of Locality of Node Mobility on Message Delivery Time

Though our method can be applied to any positional distribution p_i, we first present numerical results for the case in which the positional distribution follows a one-dimensional normal distribution as one of the simplest possible cases. We consider the case that nodes move on a one-dimensional space, and we let $p_i(x)$ be as

$$p_i(x) = \frac{1}{\sqrt{2\pi\sigma^2}} \mathrm{e}^{-\frac{(x-h_i)^2}{2\sigma^2}}. \tag{9}$$

The mean point h_i corresponds to the anchor point of node i. A smaller standard deviation σ leads to a stronger locality of node mobility since node movements are confined to a smaller area, and in this case the expectation $\mathrm{E}[L]$ of the distance L from h_i to the current node position, which represents strength of locality, is smaller: $\mathrm{E}[L] = 2\sigma/\sqrt{\pi}$. When we assume that $p_i(x)$ is given by Eq. (9), the contact frequency $w_{i,j}$ between node i and j is

$$w_{i,j} = \frac{\bar{v}}{\sqrt{\pi\sigma^2}} \mathrm{e}^{-\frac{(h_i-h_j)^2}{4\sigma^2}}.$$

We see that $w_{i,j}$ is $\Theta(\mathrm{e}^{-\delta^2})$ as a function of the distance between the anchor points $\delta = |h_i - h_j|$, so the contact frequency rapidly decays with decreasing node density.

We now change the strength of locality of node mobility by manipulating the standard deviation of the normal distribution and then comparing the resulting message delivery time and spatial distribution of infected nodes. We consider the ratio of infected nodes at time t in a DTN composed of $N = 50$ nodes. We assume average relative velocity $\bar{v}$ of nodes is 4000 [m/h] and anchor points are placed at 400 [m] intervals (i.e., $h_i = 400(i-1)$ [m]). We denote the initially infected node as node 0, and thereby $\boldsymbol{\pi}(0) = (1, 0, \ldots, 0)^T$. We set the standard deviation σ to 100 [m], 200 [m], 400 [m], 800 [m], 1600 [m], 3200 [m], and 6400 [m] and calculate the times until 50% of the nodes have become infected (50% delivery time) by using Eqs. (7) and (8). The results are shown in Figure 3. In addition to the calculation using the difference equation, we perform a Monte Carlo simulation of epidemics on the graph and thus obtain another estimate of the 50% delivery time. In the simulation, an infected node forwards a message randomly in accordance with the rate of link weights on a graph with weighted adjacency matrix A. The simulation results are shown in Figure 3 together with the results of the difference equation. We can see that the 50% delivery time is extremely long for $\sigma = 100$ [m]. The main reason for this is that infected nodes are not likely to

move into areas containing other nodes since the locality of node mobility is too strong. Though we showed the result for 50% delivery time in Figure 3, we got similar results for 25%, 75%, and 100%, which are not included in this paper due to space limitation. The difference between the results of the simulation and the difference equation is caused by the nature of the SI model as we explained in Section 3.

We also performed experiments where nodes are distributed on a two-dimensional space. We assume that the positional distribution of node follows an uncorrelated two-dimensional normal distribution with pdf $p_i(x, y)$ given by

$$p_i(x,y) = \frac{1}{\sqrt{2\pi\sigma^2}} \mathrm{e}^{-\frac{(x-h_{x,i})^2}{2\sigma^2}} \cdot \frac{1}{\sqrt{2\pi\sigma^2}} \mathrm{e}^{-\frac{(y-h_{y,i})^2}{2\sigma^2}}, \tag{10}$$

where σ and $(h_{x,i}, h_{y,i})$ denote the standard deviation and location of the mean point of the normal distribution, respectively. In this case $\mathrm{E}[L]$, which represents the strength of locality of node mobility, is $\mathrm{E}[L] = \sqrt{\pi}\sigma$. When the positional distribution of node i is given by Eq. (10), the contact frequency $w_{i,j}$ between nodes i and j is

$$w_{i,j} = \frac{r^2}{4\sigma^2 T_{\mathrm{cd}}} \mathrm{e}^{-\frac{(h_{x,i}-h_{x,j})^2+(h_{y,i}-h_{y,j})^2}{4\sigma^2}}.$$

As in the case of a one-dimensional space, the contact frequency $w_{i,j}$ is $\Theta(\mathrm{e}^{-\delta^2})$ as a function of distance between the anchor points $\delta = \sqrt{(h_{x,i} - h_{x,j})^2 + (h_{y,i} - h_{y,j})^2}$.

Changing the strength of locality of node mobility by manipulating the standard deviation of the normal distribution, we derive the message delivery time. We consider the ratio of infected nodes at time t in a DTN composed of $N = n \times n = 100$ nodes with the condition that the anchor points (mean points) $(h_{x,i}, h_{y,i})$ are placed at the grids of 10 $times$ 10 lattice, as shown in Figure 2. We set the standard deviation σ to 100 [m], 200 [m], 400 [m], 800 [m], 1600 [m], 3200 [m], and 6400 [m], and we set the other parameters to the same values as in the experiments on a one-dimensional space. From the results shown in Figure 4 we can see that the 50% delivery time is extremely long for $\sigma = 100$ [m] (we got similar results for 25%, 75%, and 100%). It is also long when σ is larger than 1600 [m]. The reason for this is that nodes spread widely, thereby losing opportunities of contacts.

4.2 Effect of the Behavior of the Tail of the Positional Distribution

In order to investigate the effect of heavy-tailed positional distributions of nodes on message diffusion, we compare the results for a Cauchy distribu-

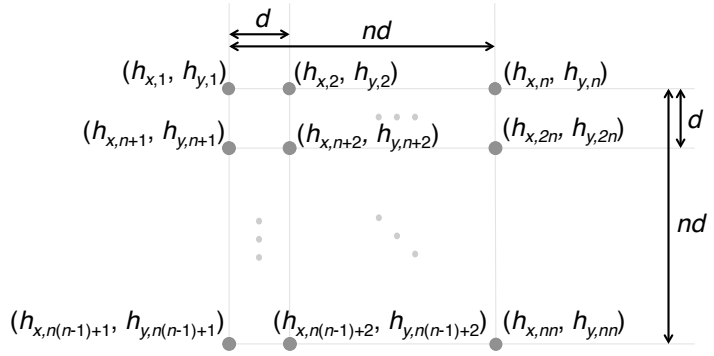

FIGURE 2
Location of anchor point $(h_{x,i}, h_{y,i})$ of node i

tion with those for a normal distribution. The behavior of the tail of the positional distribution reflecting the motion patterns of nodes strongly affects the expectation $\mathrm{E}[L]$ of the distance L from the anchor point to the current node position. The Cauchy distribution is a well-known heavy-tailed distribution [11], although its pdf is symmetric and bell-shaped, similar to that of a normal distribution. Since the tails of a Cauchy distribution are $\Theta(|x|^{-2})$ and they decay slowly, we cannot define a mean and variance, though a mode is definable. When node position follows a Cauchy distribution, $\mathrm{E}[L]$ diverges and locality of node mobility is extremely weak. In this case the positional distribution $p_i(x)$ of node i on a one-dimensional space is given by

$$p_i(x) = \frac{\mu}{\pi((x - h_i)^2 + \mu^2)}, \tag{11}$$

where μ and h_i denote the scale parameter and the coordinates of the mode (i.e., the anchor point of the node), respectively. When the positional distribution of node i is given by Eq. (11), the contact frequency $w_{i,j}$ between nodes i and j is

$$w_{i,j} = \frac{4r\mu}{\pi((h_i - h_j)^2 + 4\mu^2)}.$$

When node positions follow Cauchy distributions, contact frequency $w_{i,j}$ is $\Theta(\delta^{-2})$ as a function of the distance $\delta = |h_i - h_j|$ between the anchor points of nodes i and j.

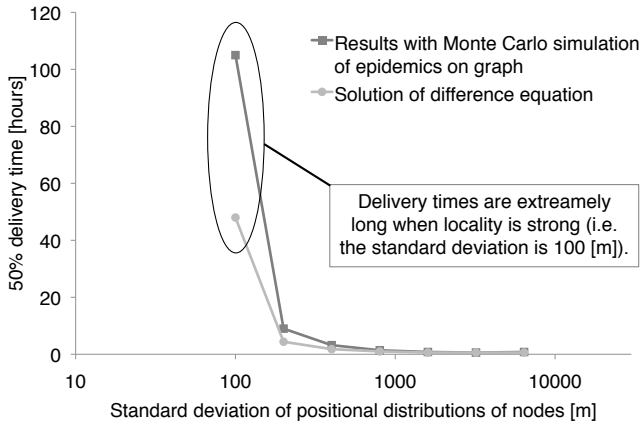

FIGURE 3
50% delivery times for different normal distributions used for the positional distributions of nodes on a one-dimensional space.

Figure 5 shows a comparison of the 50% delivery times for a Cauchy distribution (calculated by numerically solving the difference equation of Eq. (7)) and for a Monte Carlo simulation of epidemics on the graph. To make a direct comparison with the results for normal distributions, we adjust the scale parameter μ such that x_c and x_n, satisfying $F_c(x_c) = 0.9$ and $F_n(x_n) = 0.9$, take the same value, where $F_c(x)$ and $F_n(x)$ denote the cumulative distribution functions of the Cauchy and normal distributions, respectively. Therefore, the area in which a node is distributed with probability 0.8 (in other words, excluding the portions of the two tails of the distribution corresponding to a probability of 0.1 each) is the same for both distributions. We then plot the results on a horizontal axis that represents the standard deviation of the corresponding normal distribution. The other parameters are the same as in the example of a normal distribution. By comparing Figure 3 with Figure 5, we can see that although the 50% delivery time is long for the normal distribution when $\sigma = 100$ [m], the corresponding result for a Cauchy distribution is nearly the same as the results for Cauchy distributions that correspond to $\sigma = 200$ [m] and $\sigma = 400$ [m]. The main reason for this result is that, compared with a normal distribution, a Cauchy distribution gives a high probability that a node contacts another node located far from it. This is because the Cauchy distribution has a heavy tail and the locality of node

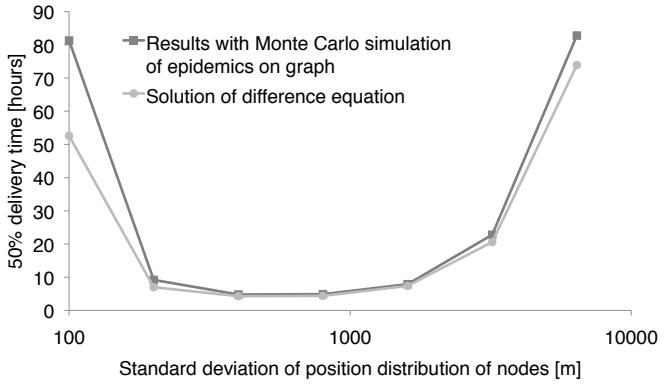

FIGURE 4
50% delivery times for different uncorrelated two-dimensional normal distributions used for the positional distributions of nodes on a two-dimensional space.

mobility is extremely weak.

Generally, if the pdf of a positional distribution of a node is $\Theta(\psi^{-\gamma})$ as a function of distance ψ from its anchor point to the current node position, the message diffusion speed is $\Theta(d^{-\gamma})$ as a function of the distance d between adjacent anchor points. Consider two nodes, i and j, on a one-dimensional space. We consider that the pdf of the position of node i is $\Theta(\psi^{-\gamma})$ (i.e., $p_i(x) = \Theta(x^{-\gamma})$ and $p_i(-x) = \Theta(x^{-\gamma})$) and the pdf of the position of node j is $p_j(x) = p_i(x - \delta)$. The contact frequency between node i and j is then

$$\begin{aligned} w_{i,j} &= \frac{2r}{T_{\mathrm{cd}}} \int_{-\infty}^{\infty} p_i(x) p_i(x - \delta) \mathrm{d}x \\ &= \frac{2r}{T_{\mathrm{cd}}} \int_{-\infty}^{\infty} p_i(x) p_i(\delta - x) \mathrm{d}x. \end{aligned}$$

So $w_{i,j} = \Theta(\delta^{-\gamma})$, since a convolution of power law functions with exponents $-\gamma_1$ and $-\gamma_2$ is a power law function with exponent $-\min(\gamma_1, \gamma_2)$ [26]. We can, therefore, understand why the contact frequency for any pair of nodes is $\Theta(d^{-\gamma})$ since $\delta = d|i - j|$.

Assuming that nodes are distributed on a two-dimensional space and node position follows a two-dimensional Cauchy distribution, we derive the 50% delivery time and compare the results with the results for a two-dimensional normal distribution. We assume that the positional distribution $p_i(x, y)$ of

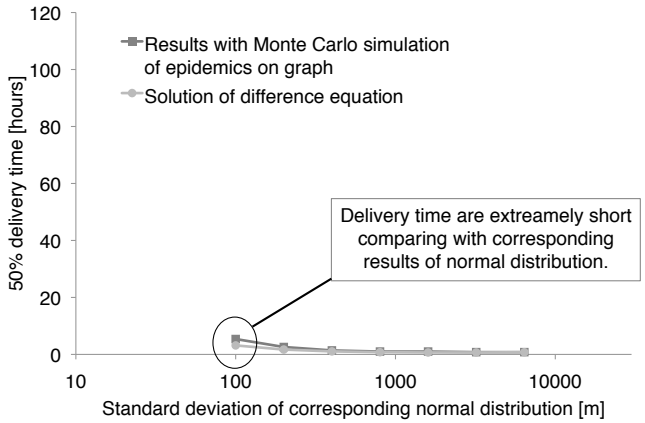

FIGURE 5
50% delivery times for different Cauchy distributions used for the positional distributions of nodes on a one-dimensional space.

node i is

$$p_i(x,y) = \frac{\mu}{\pi((x-h_{x,i})^2+\mu^2)} \cdot \frac{\mu}{\pi((y-h_{y,i})^2+\mu^2)}, \tag{12}$$

where μ and $(h_{x,i}, h_{y,i})$ denote the scale parameter and the coordinates of the anchor point (mode point), respectively. When the positional distribution of node i is given by Eq. (12), we derive the total duration of contact $T_{\rm total}$ per unit time between nodes i and j from

$$w_{i,j} = \frac{4r^2\mu^2}{\pi((h_{x,i}-h_{x,j})^2+4\mu^2)((h_{y,i}-h_{y,j})^2+4\mu^2)\,T_{\rm cd}}.$$

Figure 6 shows the 50% delivery time for a Cauchy distribution (calculated by numerically solving the difference equation of Eq. (7)) together with that for a Monte Carlo simulation of epidemics on the graph. Note that the parameter settings are the same as in the experiment for two-dimensional normal distribution. By comparing Figure 4 and Figure 6, we can see that the result for a Cauchy distribution corresponding to $\sigma = 100$ [m] is small.

Differences in tail behavior of a positional distribution also affect the spatial distribution of infected nodes. We derive the infection probability $\pi_i(t)$ of node i at 25%, 50%, and 75% delivery times for the cases that node position follows a normal and Cauchy distribution on a one-dimensional space, and the

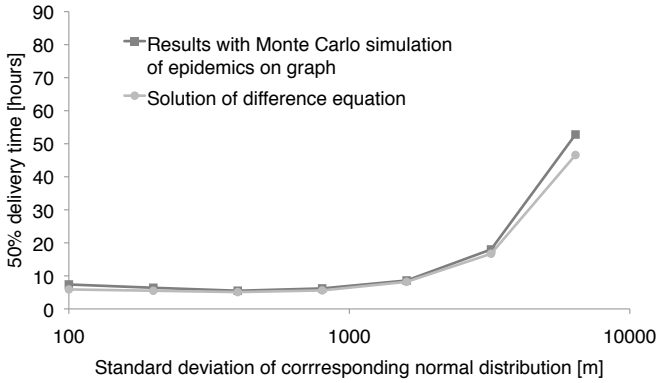

FIGURE 6
50% delivery times for different Cauchy distributions used for the positional distributions of nodes on a two-dimensional space.

results are shown in Figs. 7 and 8. In the derivations, the standard deviation of the normal distribution and the standard deviation of the normal distribution corresponding to the Cauchy distribution are 100 [m], and the conditions other than the standard deviation are the same as in the previous experiments. In Figure 7 there is a clear division between an area of infected nodes and another area: there is an *infection wall* between the two areas. This occurs because an infected node can forward a message to only nodes whose anchor points are adjacent to the anchor point of the infected node when the strength of locality of node mobility is high. In contrast, it can be seen in Figure 8 that, when node position follows a Cauchy distribution, the infection wall does not appear: messages are carried to distant areas and are widely distributed. We have also derived infection probabilities for nodes whose positions follow two-dimensional normal and Cauchy distributions at 50%delivery times. The results are shown in Figs. 9 and 10 for the normal and Cauchy cases, respectively. In the derivations, the standard deviation of the normal distribution and the standard deviation of the normal distribution corresponding to the Cauchy distribution are 100 [m], and the conditions other than the standard deviation are the same as in the previous two-dimensional experiments. The results are similar to those for the experiment on a one-dimensional space.

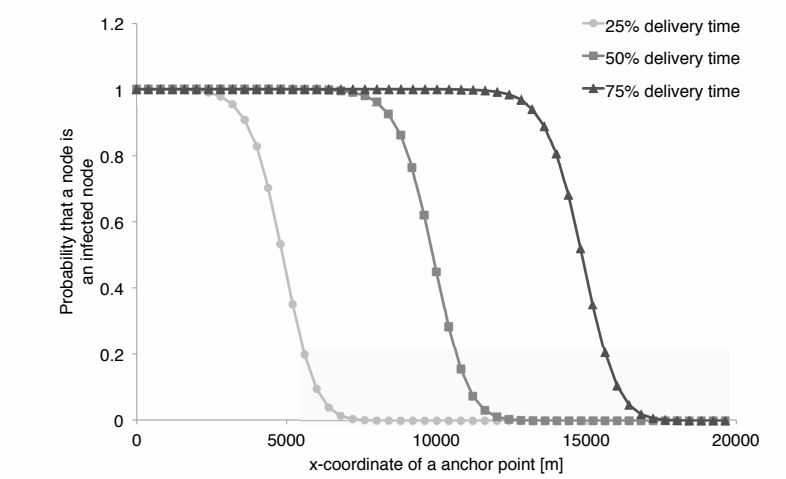

FIGURE 7
Infection probability of nodes when normal distributions are used for the positional distributions of nodes on a one-dimensional space.

5 ANALYSIS OF MESSAGE DELIVERY TIME FOR THE HLW MOBILITY MODEL

In this section, we derive the stationary positional distribution of a node that follows the HLW mobility model. As we mentioned above, the HLW mobility model is one of the few models that explicitly include locality of node mobility. We clarify the relationship between movement patterns and locality of node mobility through the derivation of message delivery time in the HLW mobility model.

5.1 Positional Distribution of a Node Following the HLW Mobility Model

The positional distribution of a node that follows the HLW mobility model varies with the parameters of the HLW mobility model. The HLW mobility model is parameterized by three numbers: the probability α that a node

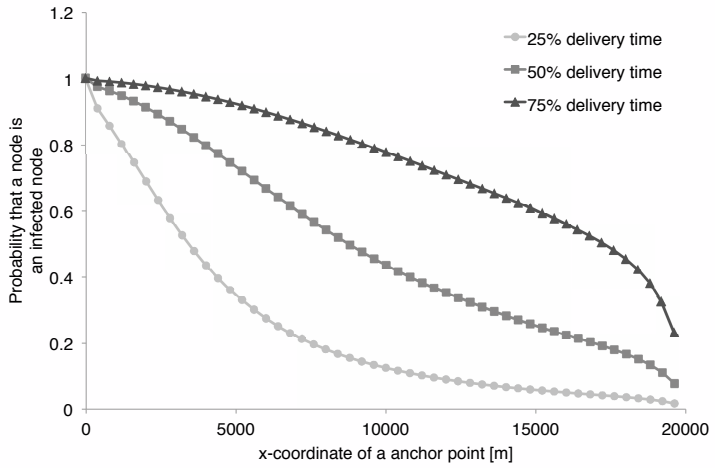

FIGURE 8
Infection probability of nodes when Cauchy distributions are used for the positional distributions of nodes on a one-dimensional space.

returns to its anchor point, the expected flight length λ, and the absolute exponent β in the pdf of flight length. The larger α is, the more a node is attracted to its anchor point, thereby increasing locality of node mobility. The longer λ is, the further a node moves from its anchor point in a small number of steps, thereby decreasing locality of node mobility. The parameter β determines the tail behavior of the positional distribution of a node. Note that λ diverges when $\beta \leq 2$.

When nodes are distributed on a one-dimensional space, the pdf for the turning point of a node is $\Theta(x^{-\beta})$. Consider a node that follows the HLW mobility model on a one-dimensional space with anchor point placed at the origin. The turning point of a node has stationary distribution when $\alpha > 0$. Denoting the pdf $f(l)$ of flight length by $\Theta(l^{-\beta})$, the pdf $p_i^s(x)$ of the turning

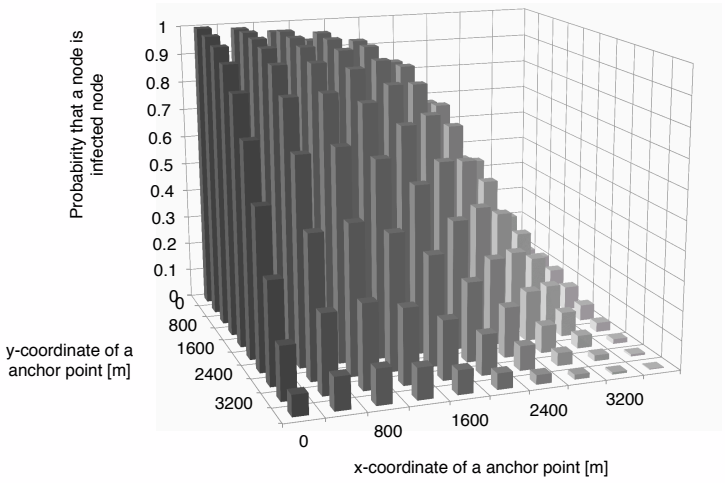

FIGURE 9
Infection probability of nodes when normal distributions are used for the positional distributions of nodes on a two-dimensional space.

point satisfies

$$p_i^s(x) = \alpha\delta(x) + (1-\alpha)\int_{-\infty}^{\infty} p_i^s(u)\frac{f(|x-u|)}{2}\mathrm{d}u,$$

where $\delta(\cdot)$ denotes the Dirac delta function. Let X_n and $p_{X_n}^s(x)$ denote a turning point after n $(n = 1, 2, \dots)$ flights without returning to its anchor point and the pdf of X_n, respectively. The pdf $p_i^s(x)$ is expressed as a linear sum of $p_{X_n}^s(x)$ and $\delta(x)$ as follows:

$$p_i^s(x) = \alpha\delta(x) + \sum_{n=1}^{\infty}(1-\alpha)^n p_{X_n}^s(x).$$

X_n is a sum of independent random variables whose pdfs are $p_{X_n}^s(x)$. Since a convolution of power law functions with exponents $-\beta_1$ (≥ -3) and $-\beta_2$ $(\geq$

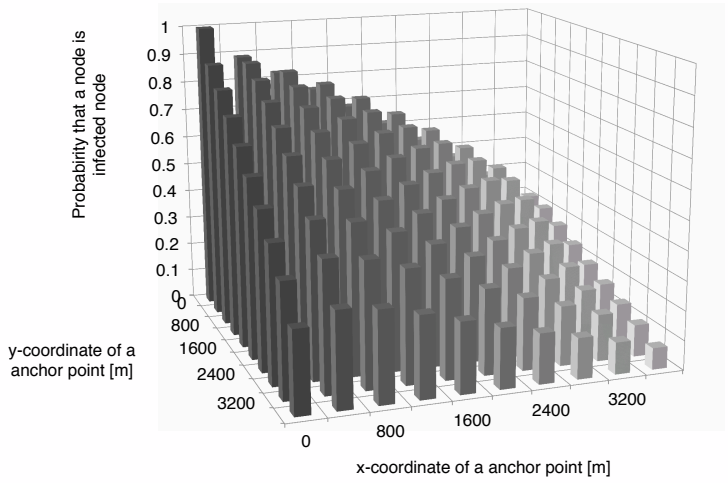

FIGURE 10
Infection probability of nodes when Cauchy distributions are used for the positional distributions of nodes on a two-dimensional space.

$-3)$ is a power law function with exponent $-\min(\beta_1, \beta_2)$ when $\beta \leq 3$ [26], we see that $p^s_{X_n}(x) = \Theta(x^{-\beta})$ and $p^s_i(x) = \Theta(x^{-\beta})$. On the other hand, when $\beta > 3$, the central limit theorem guarantees that the distribution of X_n converges to a normal distribution as $n \to \infty$. Therefore, $p^s_{X_n}(x) = \Theta(\mathrm{e}^{-x^2})$ as $n \to \infty$. As a result, $p^s_i(x) = \Theta(x^{-\beta})$ since $p^s_{X_1}(x) = \Theta(x^{-\beta})$.

Moreover, we can prove that the pdf of node position on a one-dimensional space is $\Theta(x^{-\beta+1})$ for $\alpha > 0$ and the expectation $\mathrm{E}[L]$ of the distance L from an anchor point diverges when $\beta \leq 3$. The event that node i passes an infinitesimal interval $[x, x + \mathrm{d}x)$ can be categorized into the following two types: (a) the node passes the interval while it is returning to its anchor point; (b) the node passes the interval during a flight whose length follows a power law. Letting u denote a turning point, an event of type (a) occurs with

probability α when $|x| < |u|$, and an event of type (b) occurs with probability

$$(1-\alpha)\frac{1-F(|u-x|)}{2},$$

where $F(l)$ denotes the CDF (Cumulative Distribution Function) of flight length l. Since velocity is independent of flight length and turning point, the probability that node i stays in $[x, x+\mathrm{d}x)$ is proportional to the sum of the passing probabilities. Therefore, integrating the probabilities of events (a) and (b) for turning point u, the pdf $p_i(x)$ of the position of node i is given by

$$p_i(x) = \frac{\alpha \int_{|x|}^{\infty} p_i^s(u)\mathrm{d}u + (1-\alpha)\int_{-\infty}^{\infty} p_i^s(u)\frac{1-F(|u-x|)}{2}\mathrm{d}u}{\Sigma_1}, \qquad (13)$$

where Σ_1 denotes a normalization constant. As we mentioned above, since $p_i^s(x) = \Theta(x^{-\beta})$, $\alpha\int_{|x|}^{\infty} p_i^s(u)\mathrm{d}u = \Theta(x^{-\beta+1})$. Therefore, $(1-\alpha)\int_{-\infty}^{\infty} p_i^s(u)(1-F(|u-x|))/2\,\mathrm{d}u = \Theta(x^{-\beta+1})$ since it is a convolution of $p_i^s(x) = \Theta(x^{-\beta})$ and $(1-F(|u-x|))/2 = \Theta(x^{-\beta+1})$. As a result, we find that $p_i(x) = \Theta(x^{-\beta+1})$, and $\mathrm{E}[L]$ diverges when $\beta \geq 3$. In Figure 11 we show the complementary CDFs of the position of a node that follows the HLW mobility model on a one-dimensional space for $\beta = 2.5$ and 3.5, derived by performing some simulations. The distribution of flight length is a Pareto distribution in the simulations, and α and λ are set to 0.5 and 50 [m], respectively. We added two lines with slopes of -0.5 and -1.5 to the figure. We can see that the distributions are power law distributions, and the complementary CDFs are $\Theta(x^{-\beta+2})$ (Note that, if a pdf is $\Theta(x^{-\beta+1})$, the complementary CDF is $\Theta(x^{-\beta+2})$).

On the other hand, when nodes are distributed on a two-dimensional space, the pdf of the position of a node that follows the HLW mobility model is $\Theta(x^{-\beta})$ for $\alpha > 0$, and the expectation $\mathrm{E}[L]$ of the distance L from an anchor point diverges when $\beta \leq 3$. The pdf $p_i^s(x,y)$ of the turning point of a node with anchor point placed at the origin satisfies

$$p_i^s(x,y) = \alpha\delta(x)\delta(y) + (1-\alpha)\int_{-\infty}^{\infty}\int_{-\infty}^{\infty} p_i^s(u,v)\frac{f(\phi)}{2\pi\phi}\mathrm{d}u\mathrm{d}v,$$
$$\phi = \sqrt{(x-u)^2+(y-v)^2}.$$

Since $f(\phi)/2\pi\phi = \Theta(\phi^{-\beta-1})$, $p_i^s(x,y) = \Theta(\psi^{-\beta-1})$ $(\psi = \sqrt{x^2+y^2})$, as in the one-dimensional case. Letting (u,v) denote the coordinates of a turning point, the probability of the event that a node passes a $\mathrm{d}r$-neighborhood of a

point (x, y) during a flight whose length follows a power law is

$$(1-\alpha)\frac{1-F(\phi)}{2\pi\phi/(2\mathrm{d}r)}.$$

By extending the result from the one-dimensional case, $p_i(x, y)$ is

$$\begin{aligned} p_i(x,y) = p_i(\psi) &= \frac{t_1(\psi)+t_2(\psi)}{\Sigma_2}, \\ t_1(\psi) &= \alpha\int_{\psi}^{\infty}\frac{u}{\psi}p_i^s(u,0)\mathrm{d}u, \\ t_2(\psi) &= (1-\alpha)\int_{-\infty}^{\infty}\int_{-\infty}^{\infty}p_i^s(u,v)\frac{1-F(\phi)}{2\pi\phi}\mathrm{d}u\mathrm{d}v, \end{aligned}$$

where Σ_2 denotes a normalization constant. We can see that $p_i(\psi) = \Theta(\psi^{-\beta})$ since $p_i^s(x, y) = \Theta(\psi^{-\beta-1})$ and $(1 - F(\phi))/(2\pi\phi) = \Theta(\phi^{-\beta})$. Moreover, we find that $\mathrm{E}[L]$ diverges when $\beta \geq 3$ since $2\pi\psi p_i(\psi) = \Theta(\psi^{-\beta+1})$. In Figure 12, we show the complementary CDF of the distance between the anchor point and the current position of a node by simulating node movement that follows the HLW mobility model on a two-dimensional space for $\beta = 2.5$ and 3.5. The distribution of flight length is a Pareto distribution in the simulations, and α and λ are set to 0.5 and 50 [m], respectively. We added two lines with slopes of -0.5 and -1.5 to the figure. We can see that the distributions are power law distributions, and the complementary CDFs are $\Theta(x^{-\beta+2})$.

5.2 Effect of Average Flight Length on Message Delivery Time

In the HLW mobility model, a smaller expected flight length λ leads to stronger locality of node mobility since $\mathrm{E}[L]$ is proportional to λ when $\beta > 3$. In contrast, $\mathrm{E}[L]$ diverges and the locality of node mobility becomes weak when $\beta \leq 3$, as we mentioned in the previous section. In the experiments with normal and Cauchy distributions in Section 4, we showed that smaller $\mathrm{E}[L]$ leads to a lower contact frequency of nodes, thereby significantly increasing message delivery time.

Here we compare message delivery times for epidemic broadcasting in a DTN composed of nodes that follow HLW mobility models with different expected flight lengths λ. Message delivery time is derived by performing Monte Carlo simulations and by solving the difference equation shown in Section 3. To solve the difference equation, we obtain the positional distribution $p_i(x)$ of a node by solving Eq. (13) numerically. Excluding the mobility pattern and positional distributions of nodes, the conditions of the experiment

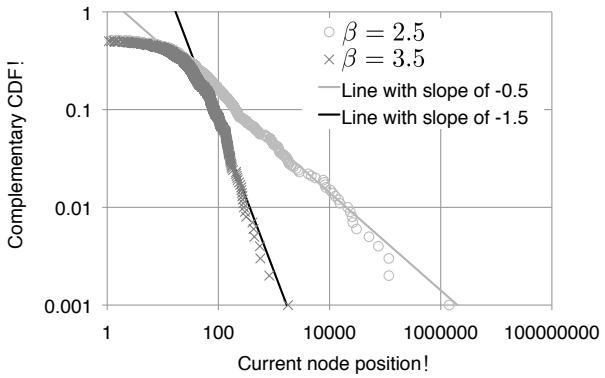

FIGURE 11
The power law appears in the positional distribution of a node that follows the HLW mobility model on a one-dimensional space.

are the same as those for the experiment on a one-dimensional space in Section 4. The parameters of the HLW mobility model are $\alpha = 0.5$ and $\beta = 2.5$ or 3.5. In Figure 13, we show the message delivery time for λ equal to 25, 50, 100, 200, 400, and 800. In the results for $\beta = 3.5$ (when $\mathrm{E}[L]$ is finite), the message delivery time increases significantly as λ decreases. In the results for $\beta = 2.5$ (when $\mathrm{E}[L]$ diverges), the message delivery time is limited. These results are consistent with the results of the experiments in Section 4.

We now consider the message delivery time for a DTN on a two-dimensional space. The conditions of the experiment are the same as those for the experiment on a two-dimensional space in Section 4. The results are shown in Figure 14. The results are similar to those of the one-dimensional version. Due to the complicated numerical computation, the solutions of difference equations in Figure 14 were obtained using $p_i(x, y)$ derived by simulation.

5.3 Effect of Power Exponent of Flight Length Distribution on Message Delivery Time

Finally, we investigate the dependency of message delivery time on the parameter β that determines the power law of flight length in the HLW mobility model. The tails of the positional distributions of nodes and the strength $\mathrm{E}[L]$ of locality of mobility depend on the parameter β, as we showed in Section 5.1. An analysis of GPS trace data indicated that the flight length of humans follows a power law with β between 1.35 and 2.40 [18].

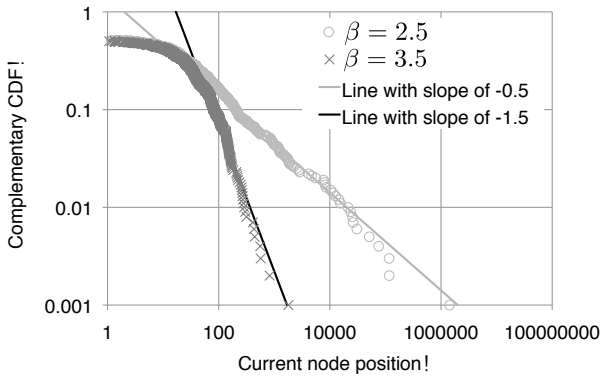

FIGURE 12
The power law appears in the distribution of distance from anchor point to current position for a node that follows the HLW mobility model on a two-dimensional space.

By changing the parameter β, we derive the message delivery time for epidemic broadcasting in a DTN composed of nodes that follow the HLW mobility model and compare the results. Message delivery time was calculated by performing Monte Carlo simulations and solving the difference equation for various values of β from 1.1 to 3.9 at intervals of 0.1. Note that we cannot analyze with fixed flight length because the expected flight length diverges when $\beta \leq 1$. In these experiments, expected flight length is set to 50 [m], and the other conditions are the same as those for the experiments described in the previous subsection. The results for one- and two-dimensional spaces are shown in Figure 15 and Figure 16, respectively. For both calculations, we find that message delivery time increases as β increases. In particular, message delivery time increases markedly when $\beta > 3$. The cause for the difference between the solutions of the difference equation and the results of Monte Carlo simulation is the limitation arising from the structure of the SI model (which we mentioned in Section 3). However, the approach using the difference equation captures the general features of message diffusion in a DTN.

As we mentioned in Section 4.2, the tail behavior of the positional distribution of a node determines the scaling law of message diffusion speed for large distances d between adjacent anchor points (i.e., when node density is extremely low). Therefore, for message diffusion on a one-dimensional

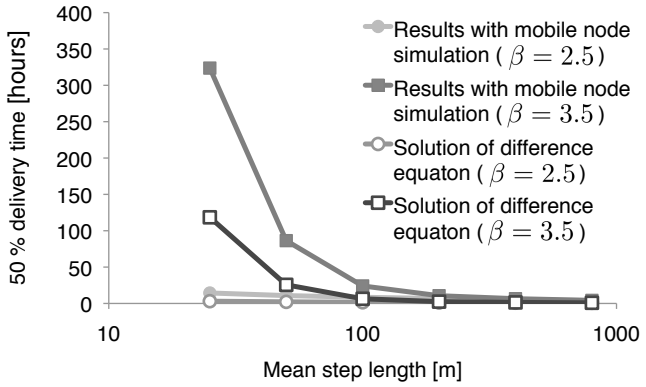

FIGURE 13
Relation between 50% delivery time in epidemic broadcasting and expected flight length λ in the HLW mobility model for a one-dimensional space.

space, with exponent β in the power law distribution of flight length, contact frequencies are $\Theta(d^{-\beta+1})$ and the time to diffuse a message is $\Theta(d^{\beta-1})$. On a two-dimensional space, contact frequencies are $\Theta(d^{-\beta})$ and the time to diffuse a message is $\Theta(d^{\beta})$.

6 CONCLUSIONS

Representing the strength of locality of node mobility through the shape of the positional distributions of nodes, we have analyzed its effect on message diffusion in epidemic broadcasting. The strength of locality of node mobility is quantified by the expectation of the distance from the mean (or mode) point to the current node position. By deriving the frequency of contact between nodes from the stationary positional distribution of the nodes, we have mapped the problem of epidemic broadcasting for mobile nodes to the problem of epidemics on a graph, and we have thus calculated message delivery time and the infection probability of nodes. Additionally, we have analyzed the effect of positional distributions of nodes on message diffusion through the numerical experiments in which we changed shape of the distribution. According to the results of the experiments, when the expectation of the distance from the mean (or mode) point to the current node position is small,

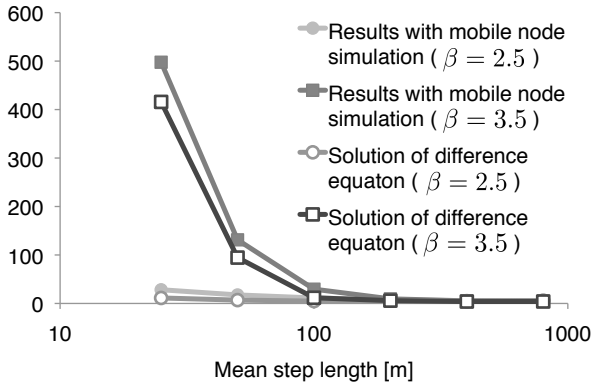

FIGURE 14
Relation between 50% delivery time in epidemic broadcasting and n expected flight length λ in the HLW mobility model for a two-dimensional space.

the message delivery time becomes extremely long and the area containing infected nodes is clearly separated from the non-infected area. On the other hand, the results showed that a difference of tail behavior of the pdf of node position has a remarkable effect on the diffusion speed in the limit of low node density. Additionally, we derived the positional distribution for the HLW mobility model, as a representative of mobility models that include locality of node mobility, and analyzed message delivery time.

Development of a locality-aware broadcast algorithm is one of future works. The results in the paper suggest that the intensity of the locality of node mobility remarkably affects the performance of broadcasting on DTNs. This means that broadcasting algorithms should be tuned depending on the intensity of locality. When the intensity of the locality is high, nodes should actively forward the message. On the other hand, the message will spread quickly, even if nodes restrain forwardings and save their resources when the locality is low. For the development of such algorithm, a mechanism to know or estimate the intensity of locality with local information is required.

ACKNOWLEDGMENTS

This work was partially supported by JSPS Grants-in-Aid for Scientific Research Number 25280030, JSPS Fellows Grant Number 24 · 3184, and Young

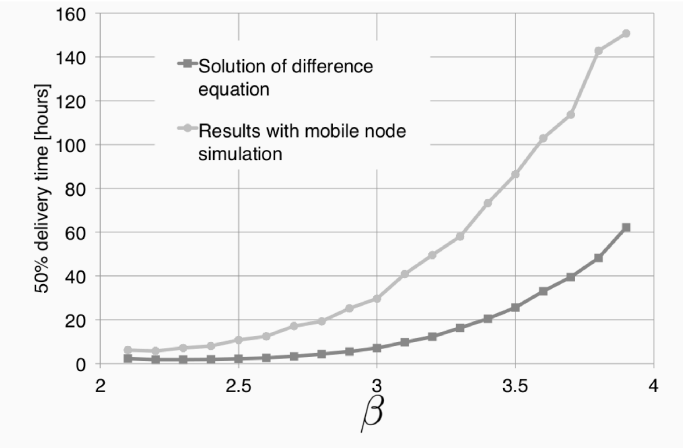

FIGURE 15
Relation between 50% delivery time in epidemic broadcasting and the absolute exponent β of the HLW mobility model on a one-dimensional space.

Scientists (Start-up) Number 26880008.

REFERENCES

[1] John Burgess, Brian Gallagher, David Jensen, and Brian Neil Levine. (April 2006). MaxProp: Routing for Vehicle-Based Disruption-Tolerant Networks. In *Proceedings of the 25th IEEE International Conference on Computer Communication (INFOCOM 2006)*, pages 1688–1698, Barcelona, Spain.

[2] Tracy Camp, Jeff Boleng, and Vanessa Davies. (September 2002). A Survey of Mobility Models for Ad Hoc Network Research. *Wireless Communications and Mobile Computing*, 2(5):483–502.

[3] Brent N Clark, Charles J Colbourn, and David S Johnson. (December 1990). Unit Disk Graphs. *Annals of Discrete Mathematics*, 86(1-3):165–177.

[4] R. J. DŚouza and Johny Jose. (February 2010). Routing Approaches in Delay Tolerant Networks: A Survey. *International Journal of Computer Applications*, 1(17):9–15.

[5] Akihiro Fujihara and Hiroyoshi Miwa. (December 2013). Homesick Lévy Walk and Optimal Forwarding Criterion of Utility-based Routing under Sequential Encounters. In Nik Bessis, Fatos Xhafa, Dora Varvarigou, Richard Hill, and Maozhen Li, editors, *Internet of Things and Inter-cooperative Computational Technologies for Collective Intelligence*, Studies in Computational Intelligence, pages 207–231. Springer.

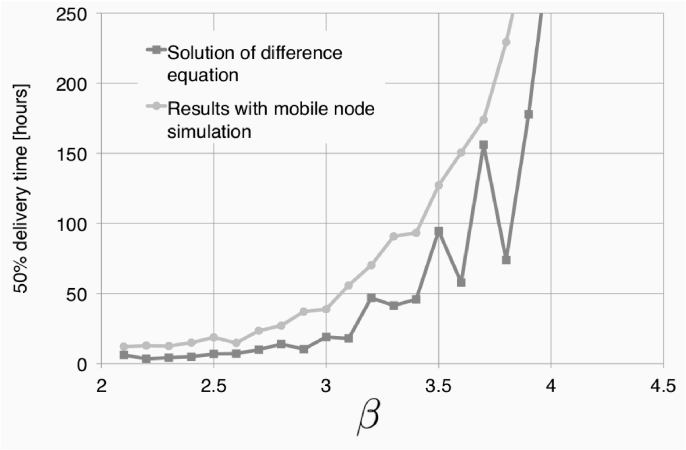

FIGURE 16
Relation between 50% delivery time in epidemic broadcasting and the absolute exponent β of the HLW mobility model on a two-dimensional space.

[6] Francesco Giudici, Elena Pagani, and Gian Paolo Rossi. (2008). Impact of Mobility on Epidemic Broadcast in DTNs. *Wireless and Mobile Networking*, 284:421–434.

[7] Francesco Giudici, Elena Pagani, and Gian Paolo Rossi. (January 2009). Self-Adaptive and Stateless Broadcast in Delay and Disruption Tolerant Networks. In *Proceedings of the 6th Italian Networking Workshop*, Cortina d'Ampezzo, Italy.

[8] Huazhi Gong and Jong Won Kim. (April 2009). A Prioritization-Based Application-Oriented Broadcast Protocol for Delay-Tolerant Networks. In *Proceedings of 2009 IEEE Wireless Communications and Networking Conference (WCNC 2009)*, pages 1–6, Budapest, Hungary.

[9] Appu Goundan, Eric Coe, and Cauligi S. Raghavendra. (November 2008). Efficient Broadcasting in Delay Tolerant Networks. In *Proceedings of 2008 IEEE Global Telecommunications Conference (GLOBECOM 2008)*, pages 1–5, New Orleans, LA, USA.

[10] David B. Johnson and David A. Maltz. (1996). Dynamic Source Routing in Ad Hoc Wireless Networks. In *Mobile Computing*, volume 353, chapter 5, pages 153–181. Kluwer Academic Publishers.

[11] Norman L. Johnson, Samuel Kotz, and N. Balakrishnan. (1994). Cauchy Distribution. In *Continuous Univariate Distributions*, chapter 16, pages 298–336. John Wiley & Sons.

[12] Uichin Lee, Soon Y. Oh, Kang-Won Lee, and Mario Gerla. (September 2009). Scaling Properties of Delay Tolerant Networks with Correlated Motion Patterns. In *Proceedings of the 15th Annual International Conference on Mobile Computing and Networking (MobiCom 2009) Workshop*, pages 19–26, Beijing, China.

[13] Yunfeng Lin, Baochun Li, and Ben Liang. (June 2008). Stochastic Analysis of Network Coding in Epidemic Routing. *IEEE Journal on Selected Areas in Communications*, 26(5):794–808.

[14] Anders Lindgren, Avri Doria, and Olov Schelén. (July 2003). Probabilistic Routing in Intermittently Connected Networks. *ACM SIGMOBILE Mobile Computing and Communications Review*, 7(3):19–20.

[15] Mark E. J. Newman. (2010). Epidemics on Networks. In *Networks an Introduction*, chapter 17, pages 627–675. Oxford University Press.

[16] Andreea Picu and Thrasyvoulos Spyropoulos. (December 2011). An Analysis of the Information Spreading Delay in Heterogeneous Mobility DTNs. Technical Report 341, Computer Engineering and Networks Lab (TIK), Swiss Federal Institute of Technology (ETH) Zurich.

[17] David Raymond, Ingrid Burbey, Youping Zhao, Scott Midkiff, and C. Patrick Koelling. (July 2006). Impact of Mobility Models on Simulated Ad Hoc Network Performance. In *Proceedings of the 9th International Symposium on Wireless Personal Multimedia Communications (WPMC 2006)*, pages 398–402, San Diego, CA, USA.

[18] Injong Rhee, Minsu Shin, Seongik Hong, Kyunghan Lee, and Song Chong. (June 2011). On the Levy-Walk Nature of Human Mobility: Do Humans Walk Like Monkeys? *IEEE/ACM Transactions on Networking*, 19(3):630–643.

[19] Elizabeth M. Royer, P. Michael Melliar-Smitht, and Louise E. Mosert. (June 2001). An Analysis of the Optimum Node Density for Ad hoc Mobile Networks. In *Proceedings of 2001 IEEE International Conference on Communications (ICC 2001)*, pages 857–861, Helsinki, Finland.

[20] Prince Samar and Stephen B. Wicker. (September 2006). Link Dynamics and Protocol Design in a Multihop Mobile Environment. *IEEE Transactions on Mobile Computing*, 5(9):1156–1172.

[21] José Santiago, Augusto Casaca, and Paulo Rogério Pereira. (January 2009). Multicast in Delay Tolerant Networks Using Probabilities and Mobility Information. *Ad Hoc & Sensor Wireless Networks*, 7(1-2):51–68.

[22] Thrasyvoulos Spyropoulos, Konstantinos Psounis, and Cauligi S. Raghavendra. (October 2004). Single-Copy Routing in Intermittently Connected Mobile Networks. In *Proceedings of the 1st IEEE Communications Society Conference on Sensor and Ad Hoc Communications and Networks (SECON 2004)*, pages 235–244, Santa Clara, CA, USA.

[23] Thrasyvoulos Spyropoulos, Konstantinos Psounis, and Cauligi S. Raghavendra. (March 2006). Performance Analysis of Mobility-Assisted Routing. In *Proceedingsthe ACM International Symposium on Mobile Ad Hoc Networking and Computing (MobiHoc 2006)*, pages 49–60, Florence, Italy.

[24] Amin Vahdat and David Becker. (July 2000). Epidemic Routing for Partially-Connected Ad Hoc Networks. Technical Report CS-2000-06, Duke University.

[25] Yunsheng Wang and Jie Wu. (July 2013). Ticket-based Multiple Packet Broadcasting in Delay Tolerant Networks. *Ad Hoc & Sensor Wireless Networks*, 19(3-4):171–188.

[26] Claus Wilke, Stephan Altmeyer, and Thomas Martinetz. (June 1998). Large-Scale Evolution and Extinction in a Hierarchically Structured Environment. In *Proceedings of the 6th International Conference on Artificial Life (ALIFE 1998)*, pages 266–274, Cambridge, MA, USA.

[27] Yosuke Yamada, Hiroyuki Ohsaki, Dimitri Perrin, and Makoto Imase. (June 2011). Impact of Mobility Constraints on Epidemic Broadcast in DTNs. In *Proceedingsthe International Conference on Complex Systems (ICCS 2011)*, pages 369–375, Tsukuba, Japan.

[28] Xiaolan Zhang, Giovanni Neglia, Jim Kurose, and Don Towsley. (July 2007). Performance Modeling of Epidemic Routing. *Computer Networks*, 51(10):2867–2891.